Proceedings of the Thirty-third (2023) International Ocean and Polar Engineering Conference **www.isope.org**
Ottawa, Canada, June 19-23, 2023

ISBN 978-1-880653-80-7; ISSN 1098-6189

Numerical Investigation of Horizontal Thermal Buoyancy Jet in Linearly Stratified Fluid

Gang Gao[1], Liushuai Cao[1], Zhiben Shen[2], Yun Wang[2], Decheng Wan[1]*

[1] Computational Marine Hydrodynamics Lab (CMHL), School of Naval Architecture, Ocean and Civil Engineering, Shanghai Jiao Tong University, Shanghai, China.
[2] Wuhan Second Ship Design and Research Institute,Wuhan,China
*Corresponding Author

ABSTRACT

In general, the thermal jet flow generated by cooling water discharge from submarine is modeled as the horizontal thermal buoyancy jet. Most of the previous experimental researches do not take the influence of density gradient into account, only a few computational investigations considered the effect of jet temperature. In this paper, a temperature-driven density stratification (TDDS) method is proposed to achieve the continuously density stratified fluid, and then implemented in the commercial software Simcenter STAR-CCM+ framework. The linear temperature distribution in the background is specified, and the relationship between density and temperature is then provided explicitly. The detached eddy simulation (DES) method based on the shear stress transport (SST) k-ω turbulence model is adopted to resolve the turbulence. Results show that stratified flow gradients affect jet trajectories. With different discharge velocity of the thermal jet, the trajectory centerlines experience two stages: the horizontal stage and the ascending stage. The jet has a larger horizonal distance with the higher Froude number. The temperature of jets decreases significantly after flowing into open water domain. As the rising height increases, the temperature of jet decay becomes very slow.

KEY WORDS:Stratified fluid, Thermal buoyancy jet, Numerical investigation, Temperature-driven density stratification, Detached eddy simulation

INTRODUCTION

Underwater vehicles occupy an important position in the military field because of their strong concealment and surprise, among which submarines are the most representative. In recent years, benefiting from the rapid development of photoelectric technology, the resolution, accuracy and anti-interference ability of infrared detection equipment have been greatly improved. It has attracted extensive attention due to its advantages such as detection. During the voyage of the underwater vehicle, the waste heat generated by its power system will be absorbed by the cooling water and discharged into the seawater along with the cooling water. The temperature of these cooling waters is significantly higher than that of the surrounding water body. Driven by the density difference, they float upwards, which may form an abnormal infrared feature on the sea surface.

At present, a large number of studies have been carried out on thermal buoyancy jet flow, and a series of achievements have been obtained. Wang et al. (2023) studied the effect of thermal jets on water surface temperature through experiments, and analyzed the influence of reynolds number, underwater depth, propeller speed and thermal jet temperature on the water surface temperature distribution. The results showed that the water surface thermal signal does not directly caused by the hot jet, but caused by the destruction of the water surface temperature distribution. The larger the jet depth and jet temperature, the larger the thermal signal area of the water surface. Li et al. (2023) used the finite volume method to establish a three-dimensional mathematical model, numerically simulated the rotation of the underwater vehicle in the background domain, analyzed the near-field and far-field cooling water trajectory and spatial evolution of the underwater vehicle, and obtained the water surface according to the distribution characteristics of temperature, it is found that when the thermal wakes on both sides rise to the water surface, an arc-shaped water surface temperature distribution area is formed. Chen et al. (2014) studied the difference in sea surface temperature distribution caused by the propeller and the submarine hull by solving the three-dimensional N-S equation. Cao et al. (2021) proposed a thermocline model for dealing with variable density stratified fluids based on the Boussinesq approximation, which solved the vortex structure and turbulent wake of blunt bodies. Huang et al. (2022) simulated the motion of a BB2 submarine model in homogeneous and linear stratified fluids, comparing drag, wake, internal wave, and free surface characteristics.

In experimental research, the thermal wake generated by cooling water discharge when the submarine is stationary is usually equivalently

simplified to a stationary horizontal thermal buoyant jet. Lou et al. (2019) simulated two merged turbulent forced plumes by solving N-S equations, and analyzed the plume velocity field and turbulent structure of two different source distances and buoyant fluxes. Yan et al. (2020) numerically simulated jet flow in a linear stratified environment using a renormalized numerical model for the discharge of wastewater in industrial and natural environments. Chen et al. (2021) used particle image velocimetry and infrared cameras to conduct experimental research on the surface temperature characteristics of thermally buoyant jets. They found that the jet evolution process can be divided into three stages, and established a prediction equation for horizontal heating. He et al. (2022) used a computational fluid dynamics model to study the flow process of a horizontal thermally buoyant jet in a linear stratified environment, and found that the rising zone of the thermally buoyant jet consists of two parts: an acceleration section and a deceleration section. The buoyancy frequency and Influence of reynolds number on thermal jet development. Ghaisas et al. (2015) analyzed the instantaneous velocity field, revealing the structure of the horizontally buoyant jet, and found that there are obvious differences in the flow near the nozzle in the stable layered region and the unstable region. Ferrari et al. (2010) conducted an experimental study of the release of an oblique negatively buoyant jet from a side hole, investigating the hydrodynamic characteristics as a function of the Froude number. Jiang et al. (2014) simulated the flow of high-temperature hydrothermal column in the deep sea, and studied the lateral and vertical development of heat flow. El-Amin et al. (2014) conducted horizontal thermal buoyancy jet experiments and numerical simulation studies, and studied the buoyancy effect on thermal jets caused by temperature differences and density changes.

According to the existing research, it can be found that in the research of horizontal thermal buoyancy jet, the effect of density gradient and the change of jet temperature are seldom considered at the same time. The chapters of this paper are arranged as follows: First, the evolution process of the thermal jet shape under typical working conditions is analyzed, the centerline of the thermal jet trajectory is defined, and the temperature change of the thermal jet is analyzed. Afterwards, the temperature and trajectory changes at different jet velocities are compared. Finally, the temperature and trajectory changes of the jet under different stratification intensities are compared.

NUMERICAL METHODS

Governing Equation

In the solution process of this paper, the fluid motion satisfies the mass conservation and momentum conservation equations.

$$\nabla \cdot \mathbf{U} = 0 \tag{1}$$

$$\frac{\partial \rho \mathbf{U}}{\partial t} + \nabla \cdot (\rho \mathbf{U}\mathbf{U}) = -\nabla p + \rho g + \nabla \cdot (\mu \nabla \mathbf{U}) \tag{2}$$

where **U** is the velocity field, ρ is the density of fluid, p is the pressure field, g is the gravity acceleration, μ is the dynamic viscosity coefficient. Turbulence model using $SST\, k-\omega$ model, Free surface capture using VOF method with artificial compressibility term, the VOF transport equation is as follows:

$$\frac{\partial \alpha}{\partial t} + \nabla \cdot (\mathbf{U}\alpha) + \nabla \cdot [\mathbf{U_r}(1-\alpha)\alpha] = 0 \tag{3}$$

U_r is the velocity field used to compress the interface, α is the volume fraction of the two-phase fluid, and represents the percentage of the volume occupied by the liquid part. The value range is 0~1, 0 represents air, 1 represents water, and between 0 and 1 is free surface position.
In order to realize the linear distribution of density, this paper needs to solve the energy equation, and realize the linear distribution of density by controlling the linear distribution of temperature.

$$\frac{\partial(\rho T)}{\partial t} + \nabla \cdot \left(\rho \vec{u} T\right) = \nabla \cdot \left(\frac{k}{c} \nabla (T)\right) + S_T \tag{4}$$

As shown in formula (4), $\frac{\partial(\rho T)}{\partial t}$ represents the local change rate of the temperature field, $\nabla \cdot \left(\rho \vec{u} T\right)$ is the thermal convection term, $\nabla \cdot \left(\frac{k}{c} \nabla (T)\right)$ is the thermal diffusion term, and S_T is the source term. Neglecting the influence of thermal radiation, expressing the density as a function of temperature, given the upper and lower temperature distributions of the layered area, the corresponding density distribution can be calculated.

SOLVERS SETUP

Geometric Model and Simulation Setup

The calculation area of the numerical simulation is shown in figure 1. The radius of the jet pipe is 0.00185 m, the length of the jet pipe is 0.4 m, the distance between the outlet of the calculation domain and the nozzle of the jet is 1.1 m, the position of the axis of the outlet of the jet pipe is the origin of coordinates, and the left and right sides of the calculation domain are both sides are 0.2m away from the pipeline axis, the bottom of the calculation domain is 0.18m away from the axis, the free liquid surface is 0.12m away from the axis, and the free surface is 0.28m away from the top of the calculation domain.

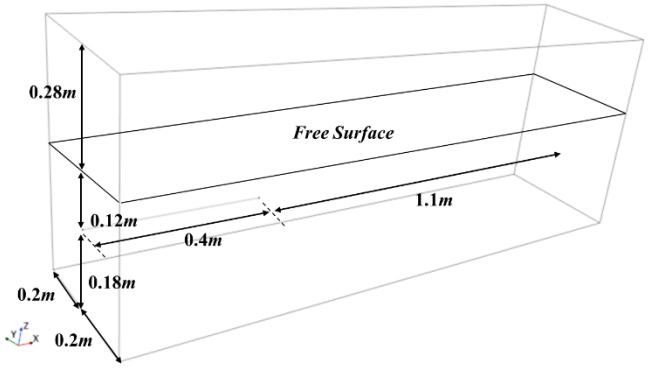

Fig. 1. Computational domain

Grid Generation

In the setting of the calculation domain, the influence of the free surface is considered, and the position of the pipe outlet is the core area of the development of the heat jet, and the grid quality will affect the distribution of the entire heat jet flow field. Therefore, at the position of the pipe exit and the position of the free surface.Encryption processing

is carried out, and the circular pipe is partially encrypted.

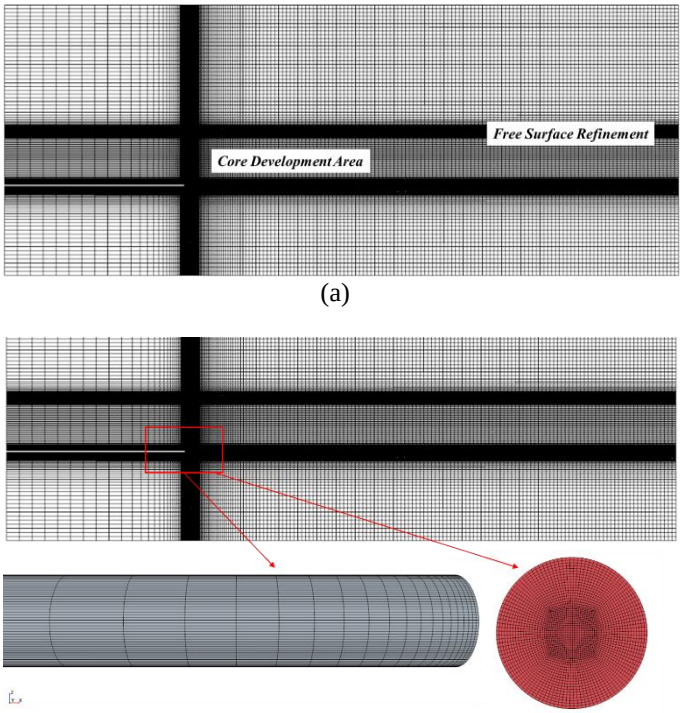

(a)

(b)

Fig. 2. Computational grids

Boundary Setting and Discretization Format

The left side of the calculation domain is set as the inlet boundary condition, and the position of the outlet of the pipeline is also set as the inlet boundary condition. The velocity of the heat jet changes accordingly. The right side of the calculation domain is set as the outlet boundary condition, and the front and back of the calculation domain are set as symmetrical boundary conditions. The upper and lower sides of the domain are set as velocity inlet boundary conditions, and the rest of the surfaces are set as free-slip walls.

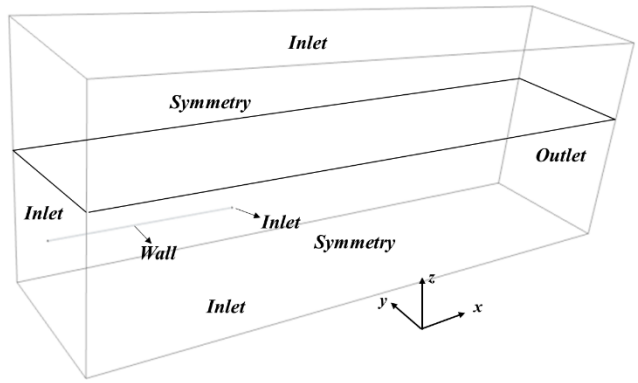

Fig. 3. Boundary condition settings

Condition Setting

An important parameter of the thermal buoyancy jet is the Froude number,

$$Fr = U_0 / \left(g_0'\right)^{1/2} \tag{5}$$

$g_0' = \left(\rho_0 - \rho_a\right) g / \rho_0$, ρ_0 is the density of the ambient water body, ρ_a is the initial density of the hot jet, Q is the thermal jet flow rate, ρ_{top} and ρ_{bottom} are the liquid densities of the uppermost and lowermost layers in the computational domain, respectively, T_{jet} is the temperature of the heat jet at the initial moment.

Table 1. Test conditions

Cases	Q(cm^3/s)	ρ_{top}(kg/m^3)	ρ_{bottom}(kg/m^3)	ρ_0(kg/m^3)	Fr	T_{jet}(℃)
1	2.1	997.61	1011.08	1003.00	11.07	35.2
2	4.2	997.61	1011.08	1003.00	22.14	35.2
3	6.3	997.61	1011.08	1003.00	33.21	35.2
4	8.4	997.61	1011.08	1003.00	44.28	35.2
5	2.1	997.61	1051.61	1019.21	23.66	35.2
6	2.1	997.61	1132.61	1051.61	10.49	35.2
7	2.1	997.61	1267.61	1105.61	7.02	35.2

The temperature and density distribution at the initial time under the first working condition is shown in the figure4.

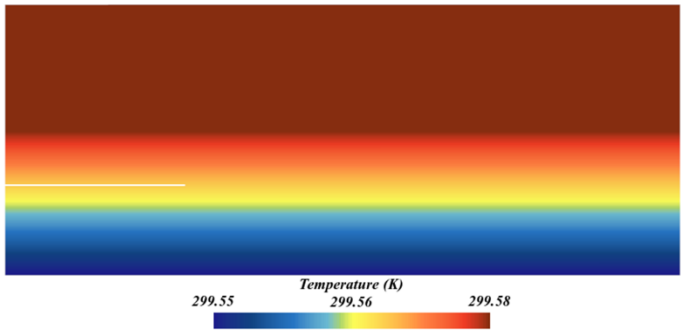

(a)

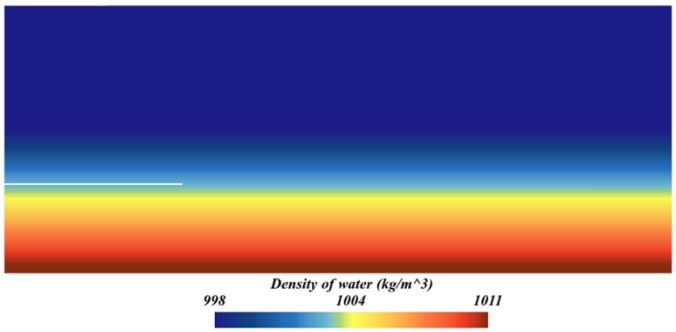

(b)

Fig. 4. Physical field distribution at initial time

The vertical distribution of density and temperature in working conditions 4-7 are shown in Figure 5.

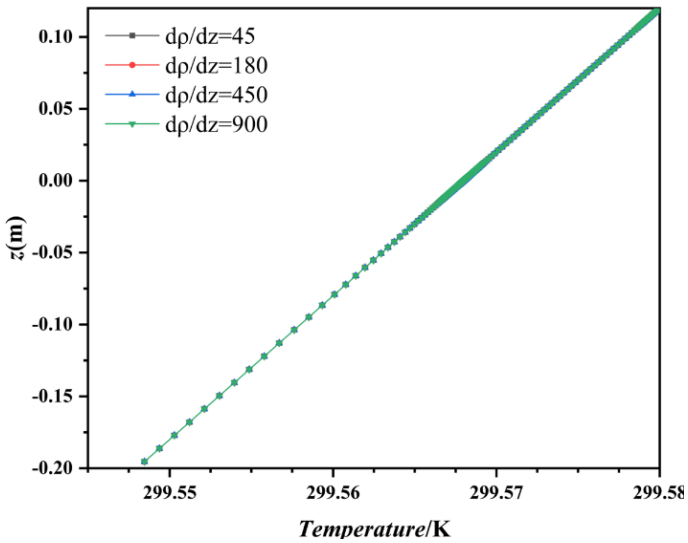

(a) Temperature distribution along the vertical direction

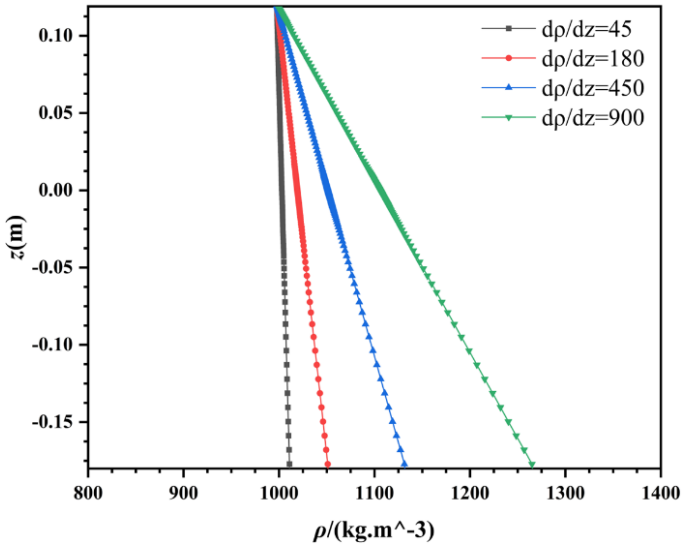

(b) Density distribution along the vertical direction

Fig. 5. Vertical variation curve of temperature and density

According to Figure 5, it can be seen that temperature and density are linearly distributed vertically, according to Table 1 and Figure 5, under working conditions 1, 2, 3, and 4 where the density gradient and jet temperature remain constant, the effects of velocity on the jet are mainly compared. Under working conditions 1, 5, 6, and 7 where the jet velocity and jet temperature remain constant, the effects of density gradient on the jet are mainly compared.

RESULTS AND DISCUSSION

Evolution Process of Jet Shape

Figure 6 shows the typical velocity and temperature fields on the symmetry plane. It can be seen that the center line coincides with the trajectory of the maximum velocity and maximum temperature on the computational domain plane.

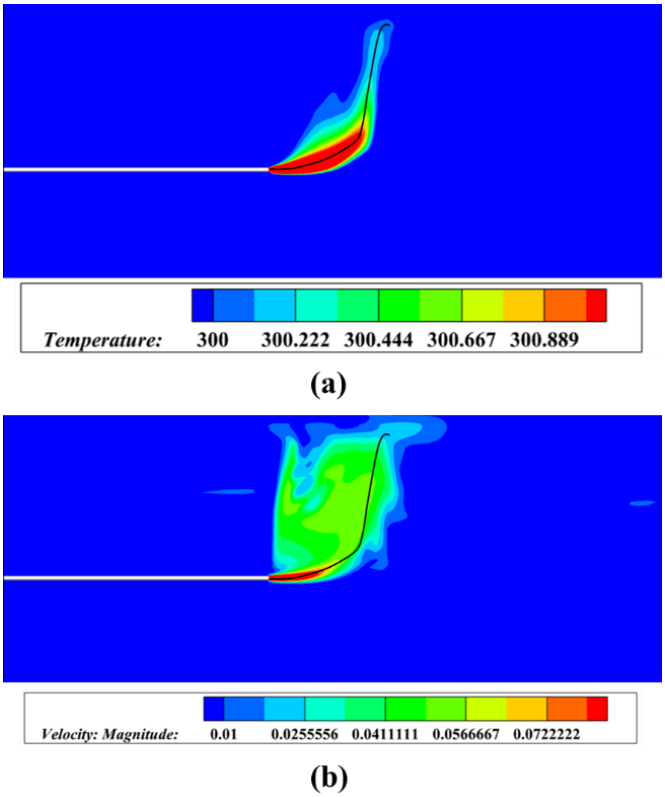

Fig. 6. Temperature and velocity distributions on a symmetrical interface

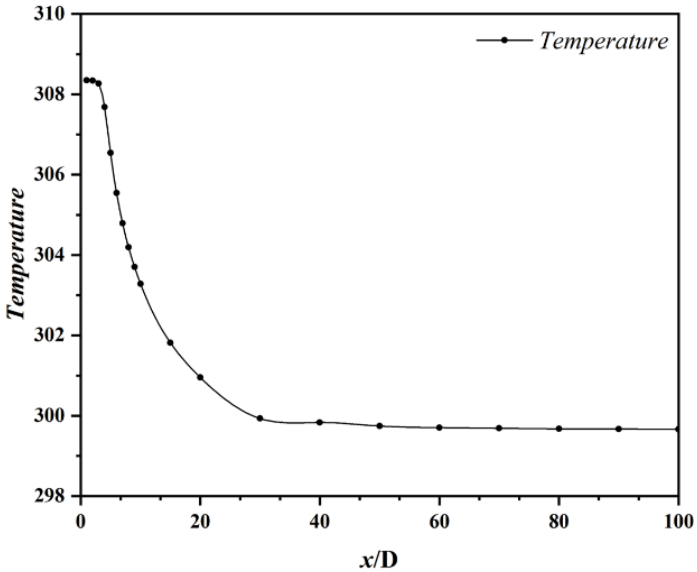

Fig. 7. Curve of temperature variation

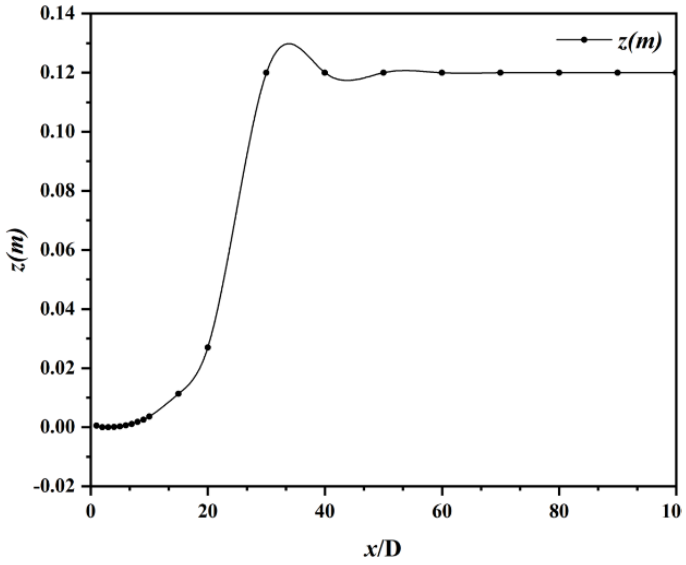

Fig. 8. Curve of track change

When the buoyant jet reaches the water surface, it will form a stable flow pattern after a certain period of time. For the thermal buoyant jet in a steady state, the maximum jet temperature points at different positions of the nozzle are extracted, with the nozzle as the coordinate origin, the ratio of the horizontal direction to the diameter D as the horizontal axis, and the temperature is on the vertical axis. The temperature change curve of the thermal buoyancy jet is obtained, as shown in Figure 7. It can be seen that when the distance from the nozzle is relatively short, the temperature of the thermal jet decays quickly, and when the distance is far away, the temperature attenuation is very slow, indicating that when the jet is close to the nozzle, the heat jet is affected by the horizontal momentum and strongly interacts with the surrounding water body to exchange heat. Extract the maximum jet temperature points at different positions of the nozzle to obtain a relatively complete thermal buoyancy jet trajectory, take the nozzle as the origin of coordinates, the ratio of the horizontal direction to the diameter D as the horizontal axis, and the vertical z direction as the vertical axis, the coordinate trajectory of the center line of the thermal buoyant jet is shown in Figure 8. It can be seen that, as previously analyzed, the trajectory of the thermal jet can be divided into a non-buoyancy zone, a transition zone, and a plume zone.

Figure 9 shows the evolution process of the thermal buoyancy jet in the working condition. The horizontal thermal buoyancy jet can be divided into three regions as a whole, namely the non-buoyancy region, the transition region and the plume region. The flow characteristics of the three stages are mainly related to the horizontal jet flow. The momentum flux is related to the buoyancy flux caused by heat. At the beginning of the flow process, the horizontal momentum flux of the hot jet is much larger than the buoyancy flux, and its flow characteristics are similar to the horizontal jet. This section is called the non-buoyancy zone. After the jet head at this stage, due to the effect of resistance, the movement speed of the jet head decreases, the effect of initial momentum gradually decreases, the effect of buoyancy increases, and the flow transitions from the effect of initial momentum to the effect of buoyancy. Called the intermediate transition zone, while the jet spreads downstream, its head has risen to the surface. In this stage, the flow gradually becomes a movement dominated by buoyancy, and its flow characteristics are close to the plume flow. This section is called the plume region.

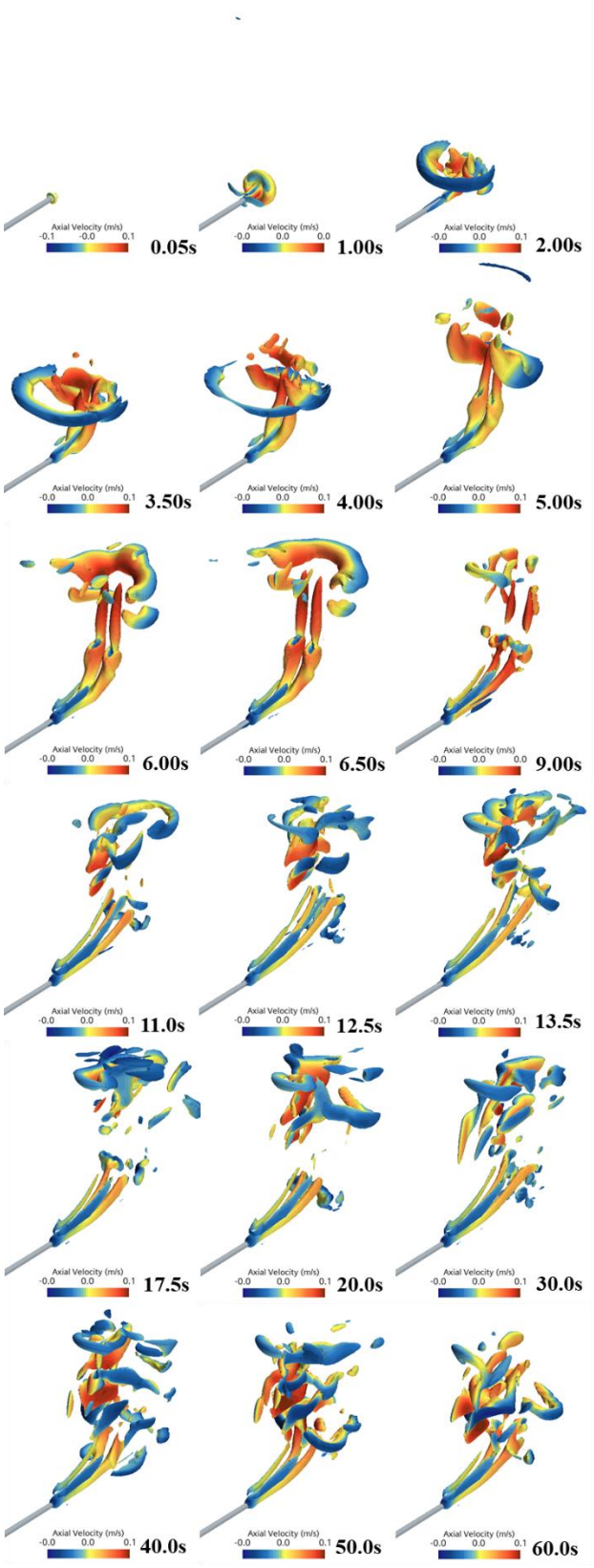

Fig. 9. Evolution process of jet vortex structure

Effect of Velocity on Jet Evolution

It can be seen from Fig. 10 that when the submerged depth, jet tube diameter and initial jet temperature remain unchanged, the trajectory centerline of the thermally buoyant jet is closely related to the Froude number. The results show that the lower the Froude number, the shorter the distance of the horizontal section of the thermally buoyant jet, the smaller the range of the non-buoyancy area; at the same time, the faster and more obvious rise of the jet center trajectory also makes the range of the plume area larger. Figure 11 shows the jet temperature change curves under different working conditions. When the submerged depth, jet tube diameter and jet initial temperature are constant, as the jet velocity increases, the center line of the hot jet trajectory rises more slowly, which is different from the surrounding water body. The slower the heat exchange, the slower the temperature decay of the hot jet.

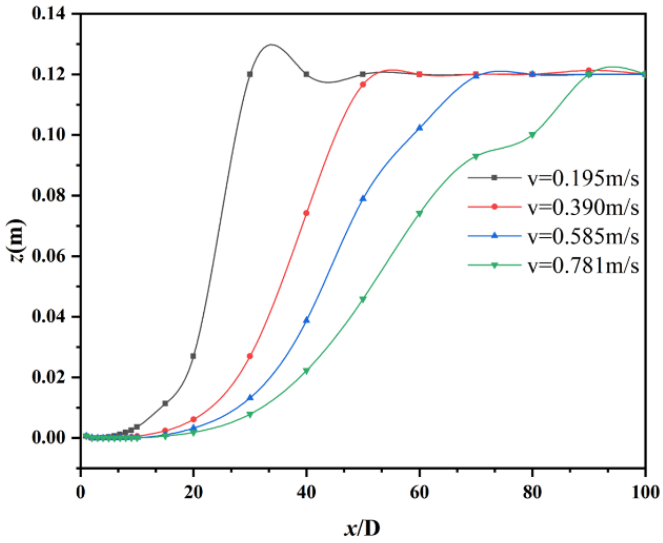

Fig. 10. Curve comparison of track change

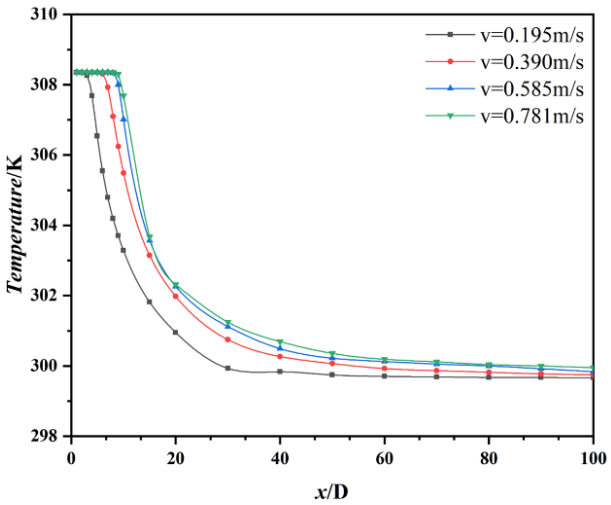

Fig. 11. Comparison curve of temperature change

Figure 12 shows the structure diagram of the jet vortex under different working conditions. It can be seen from Figure 11 that as the jet velocity increases, the horizontal development distance of the jet becomes longer, and the vertical development is suppressed.

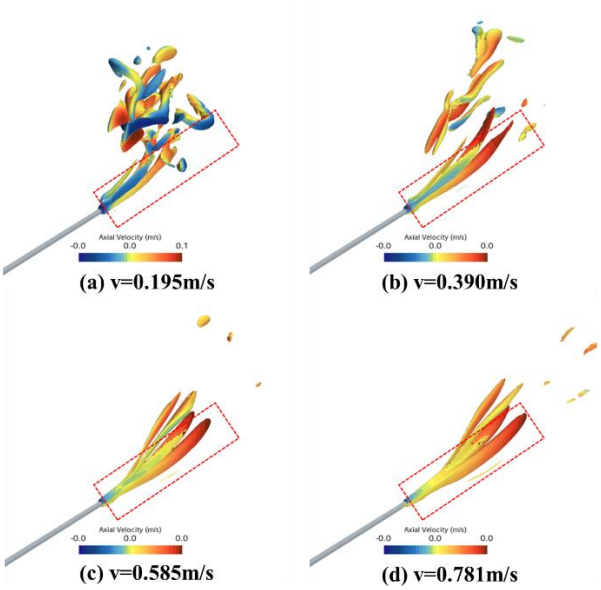

Fig. 12. Comparison of vortex structure morphology

Effect of Stratification Gradient on Jet Evolution

Figure 13 shows the change of the center line of the hot jet trajectory under different stratification intensities. As the previous analysis, as the delamination strength increases, the buoyancy of the thermal buoyancy jet is strengthened by buoyancy, and the center line of the trajectory rises faster. The scope of the non-buoyancy zone becomes smaller, and the scope of the plume zone becomes smaller. Correspondingly, the temperature change curve of the thermal jet under different stratification intensities is given. It can be seen from Fig. 14 that as the stratification intensity increases, the jet rises faster, the interaction between the thermal jet and the surrounding water body is more intense, and the temperature of the thermal jet decays faster.

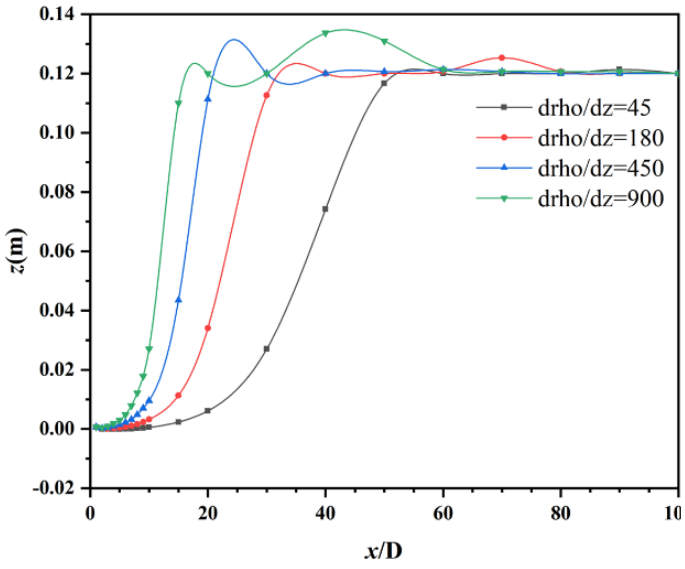

Fig. 13. Curve comparison of track change

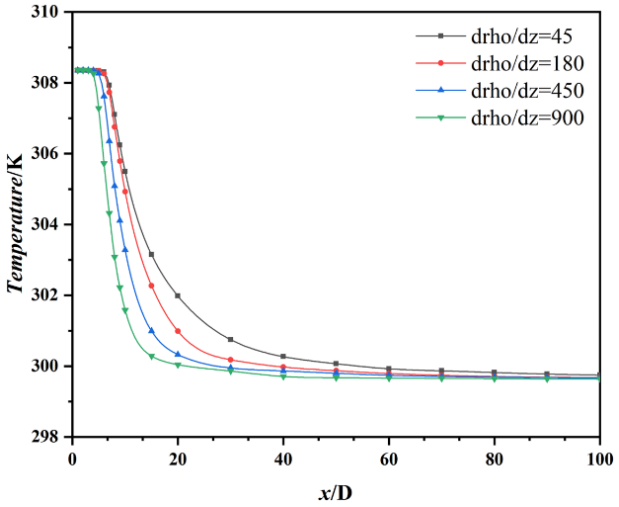

Fig. 14. Comparison curve of temperature change

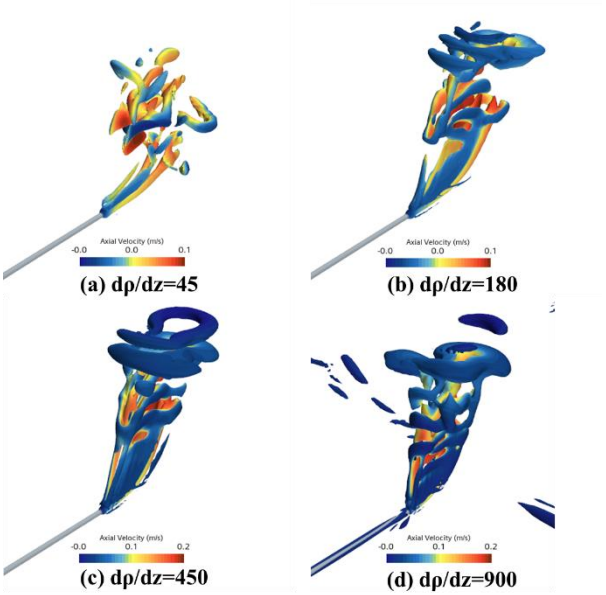

Fig. 15. Comparison of vortex structure morphology

Figure 15 shows the cloud diagram of the jet vortex structure under different stratification intensities. It can be seen that as the stratification intensity increases, the buoyancy effect of the jet after it flows out of the nozzle is obviously strengthened, and the range of the non-buoyancy area becomes smaller. The thermal buoyancy jet rises faster, the range of the non-buoyancy area becomes smaller, and the momentum loss becomes smaller.

CONCLUSIONS

In this paper, a temperature-driven density stratification (TDDS) method is proposed to achieve the continuously density stratified fluid, and then implemented in the commercial software Simcenter STAR-CCM+ framework. The linear temperature distribution in the background is specified, and the relationship between density and temperature is then provided explicitly. The detached eddy simulation (DES) method based on the shear stress transport (SST) k-ω turbulence model is adopted to resolve the turbulence.

(a) The horizontal thermal buoyancy jet can be divided into three regions as a whole, namely the non-buoyancy region, the transition region and the plume region. As the distance from the nozzle is farther away, the jet temperature gradually decays.

(b) The lower the Froude number, the faster the rise of the center line of the hot jet trajectory, the smaller the range of the non-buoyancy area, the larger the range of the plume area, and the faster the temperature decay.

(c) The greater the stratification intensity of the water body, the stronger the buoyancy effect on the thermal jet, and the faster the rise of the center line of the thermal jet trajectory. As the stratification intensity increases, the faster the temperature of the thermal jet decays.

ACKNOWLEDGEMENTS

This work was supported by the National Natural Science Foundation of China (52001210,52131102), and the National Key Research and Development Program of China (2019YFB1704200), to which the authors are most grateful.

REFERENCES

Cao, L. S., Huang, F. L., Liu, C., & Wan, D. C. (2021). Vortical structures and wakes of a sphere in homogeneous and density stratified fluid. Journal of Hydrodynamics, 33(2), 207-215.

Chen, S., Zhong, J., & Sun, P. (2014). Numerical simulation and experimental study of the submarine's cold wake temperature character. Journal of Thermal Science, 23(3), 253-258.

Chen, Y., He, Z., Lou, Y., Zhang, H., Zhu, R., & Okon, S. U. (2021). Experimental study of horizontal heated buoyant jets in a linearly stratified ambience. Physics of Fluids, 33(4), 047116.

El-Amin, M. F., Shuyu, S. U. N., & Salam, A. (2014). Simulation of buoyancy-induced turbulent flow from a hot horizontal jet. Journal of Hydrodynamics, Ser. B, 26(1), 104-113.

Ferrari, S., & Querzoli, G. (2010). Mixing and re-entrainment in a negatively buoyant jet. Journal of Hydraulic Research, 48(5), 632-640.

Ghaisas, N. S., Shetty, D. A., & Frankel, S. H. (2015). Large eddy simulation of turbulent horizontal buoyant jets. Journal of Turbulence, 16(8), 772-808.

He, Z., Zhang, H., Chen, Y., Okon, S. U., & Lou, Y. (2022). Hydrodynamics of horizontal heated buoyant jet in linearly stratified fluids. Physics of Fluids, 34(2), 025108.

Huang, F., Meng, Q., Cao, L., & Wan, D. (2022). Wakes and free surface signatures of a generic submarine in the homogeneous and linearly stratified fluid. Ocean Engineering, 250, 111062.

Jiang, H., & Breier, J. A. (2014). Physical controls on mixing and transport within rising submarine hydrothermal plumes: A numerical simulation study. Deep Sea Research Part I: Oceanographic Research Papers, 92, 41-55.

Li, G., Du, Y., & Yang, L. (2023). Simulation Study on Thermal Wake Characteristics of Underwater Vehicle under Rotary Motion. Applied Sciences, 13(3), 1531.

Lou, Y., He, Z., Jiang, H., & Han, X. (2019). Numerical simulation of two coalescing turbulent forced plumes in linearly stratified fluids. Physics of Fluids, 31(3), 037111.

Wang, C. A., Xu, D., & Gao, J. P. (2023). Surface temperature characteristics of underwater thermal jet based on thermal skin. Applied Ocean Research, 130, 103411.
Yan, X., Mohammadian, A., & Chen, X. (2020). Numerical modeling of inclined plane jets in a linearly stratified environment. Alexandria Engineering Journal, 59(3), 1857-1867.